Final Report to the U.S. Department of Energy's Program for
DOE Cooperative Agreement Number DE-SC0008459

Supported under the Office of Biological and Environmental Research Program

Collaborative Project: High-resolution Global Modeling of the Effects of Subgrid-Scale Clouds and Turbulence on Precipitating Cloud Systems

Principal Investigator: David A. Randall

Funding period: 08/15/2012 - 08/14/2015

Department of Atmospheric Science
Colorado State University
Fort Collins, Colorado 80523

tel: (970) 491-8474
email: randall@atmos.colostate.edu

*Other Senior Personnel: *Denotes Collaborating Institutions*

Peter Bogenschutz
National Center for Atmospheric Research
bogensch@ucar.edu
phone: (303) 497-1341

*Anning Cheng
Science Systems and Applications, Inc.
anning.cheng@nasa.gov
phone: (757) 864-2591

Grant Firl
Department of Atmospheric Science
Colorado State University
grant@atmos.colostate.edu
phone: (970) 491-8346

*Steven Ghan
Pacific Northwest National Laboratory
Steve.Ghan@pnnl.gov
phone:(509) 372-6169

*Marat Khairoutdinov
School of Marine & Atmospheric Sciences
SUNY at Stony Brook- Room S105 annex
Stony Brook, NY 11794-5000
phone: (631) 632-6339

*Steven Krueger
Department of Atmospheric Sciences
University of Utah
steven.krueger@utah.edu
phone: (801) 581-3903

*Vincent Larson
Department of Mathematical Sciences
University of Wisconsin at Milwaukee
vlarson@uwm.edu
phone: (414) 229-5490

*Chin-Hoh Moeng
National Center for Atmospheric Research
moeng@ucar.edu
phone: (303) 497-8911

Submitted November 2015

Intellectual Property

The intellectual property produced by our project includes equation systems, computer software, and model output, as well as publications. There are no patents. Our work has been carried out with the intention of sharing all of our results with the scientific community at large.

Abstract

We proposed to implement, test, and evaluate recently developed turbulence parameterizations, using a wide variety of methods and modeling frameworks together with observations including ARM data.

We have successfully tested three different turbulence parameterizations in versions of the Community Atmosphere Model: CLUBB, SHOC, and IPHOC. All three produce significant improvements in the simulated climate. CLUBB will be used in CAM6, and also in ACME. SHOC is being tested in the NCEP forecast model.

In addition, we have achieved a better understanding of the strengths and limitations of the PDF-based parameterizations of turbulence and convection.

Summary of Accomplishments

1. Overview

As described in some of our publications (listed later in this report), we have successfully tested three different turbulence parameterizations in versions of the Community Atmosphere Model: CLUBB, SHOC, and IPHOC. All three produce significant improvements in the simulated climate.

In addition, we have achieved a better understanding of the strengths and limitations of the PDF-based parameterizations of turbulence and convection.

2. Project description from the proposal

We proposed to implement, test, and evaluate recently developed turbulence parameterizations, using a wide variety of methods and modeling frameworks together with observations including ARM data. The parameterizations have been compared and evaluated on the basis of: their a priori conceptual merits, including closure assumptions; the realism of the results obtained in tests, including tests with global models; and their computational speeds. We have also done some modest development work to take advantage of what we have learned from our tests.

Through the proposed research, we have arrived at an understanding of the relative strengths and weaknesses of each parameterization. Our work has resulted in significant improvements to all four parameterizations, and a more widespread adoption of the parameterizations by the climate modeling community. Finally, our work has produced improved versions of the Community Atmosphere Model and its super-parameterized counterpart.

In the following sections, we report progress on a variety of different areas.

3. THOR

One of the unique features of THOR is that it includes the effects of subgrid scale ice

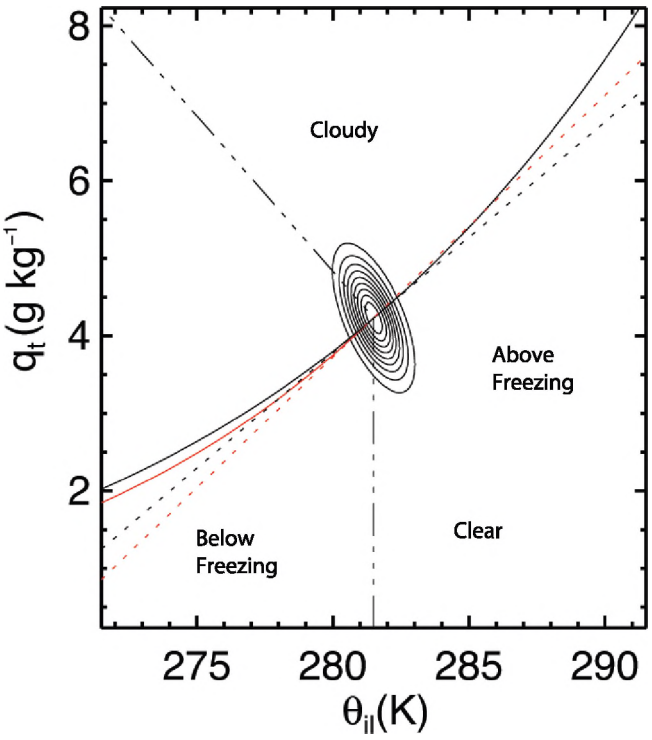

Fig. 1: Schematic illustration of the joint distribution of liquid-ice water potential temperature (horizontal axis) and total water mixing ratio (vertical axis), for the simplified case of a single Gaussian. The lines show the saturation mixing ratio over liquid (black solid), over ice (red solid), and a linear approximation to the saturation mixing ratio over liquid (black dotted), land a inear approximation to the saturation mixing ratio over ice (red dotted). The black dash-dotted lines show the liquid-ice water potential temperature at the freezing point.

clouds and mixed-phase clouds. An example is shown in Fig. 1.

We have developed a very simple method to diagnose all of the parameters of a double-Gaussian PDF from the statistics of a large-eddy simulation. An example is shown in Fig. 2.

Additional results were published by Firl and Randall (2014). Two additional papers are in

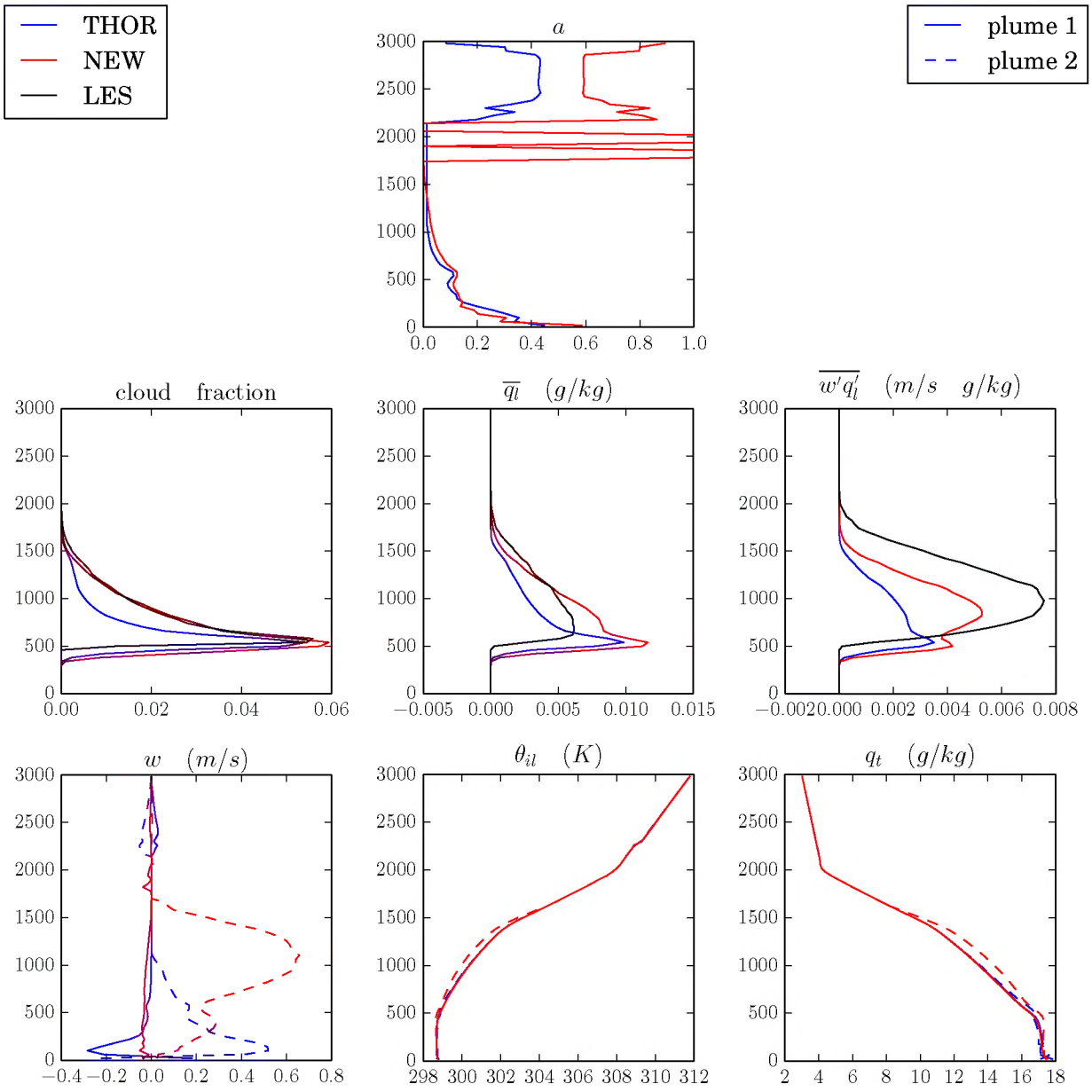

Fig. 2: Diagnostic test of the equations used in THOR, using an LES simulation of shallow cumulus convection. “Plume 1” and “Plume 2” refer to the two Gaussians. By convention, Plume 2 has larger (more positive) mean vertical motion than Plume 1. The top panel shows the vertical profile of a, the weight assigned to Plume 2. The results are meaningless above a height of about 1200 m, where the turbulence stops. In the remaining six panels, the black curves show the LES results. The blue and red curves show results obtained with older and newer versions of THOR, respectively. The new results are in better agreement with the LES.

preparation.

4. SHOC

Our overall goal during the first year was to further investigate the impacts and capabilities of SHOC (Simplified Higher-Order Closure; Bogenschutz and Krueger, 2013) as implemented in a 3D cloud-resolving model, SAM (System for Atmospheric Modeling), by simulating (1) radiative-convective equilibrium (RCE), (2) the M3CE IOP at the SGP, and (3) a cold-air outbreak case.

We performed a series of RCE simulations to study self-aggregation of convection with and without SHOC for various horizontal grid sizes. Simulations with SHOC aggregate more readily than identical simulations without SHOC. This result supports the view that self-aggregation in CRM simulations is not encouraged by using an inadequate SGS turbulence parameterization.

We prepared SAM files for a cold-air outbreak case simulation as part of the Grey Zone Project (http://appconv.metoffice.com/cold air outbreak/constrain case/home. html). These simulations have not been performed yet.

We performed a series of M3CE simulations with and without SHOC for various horizontal

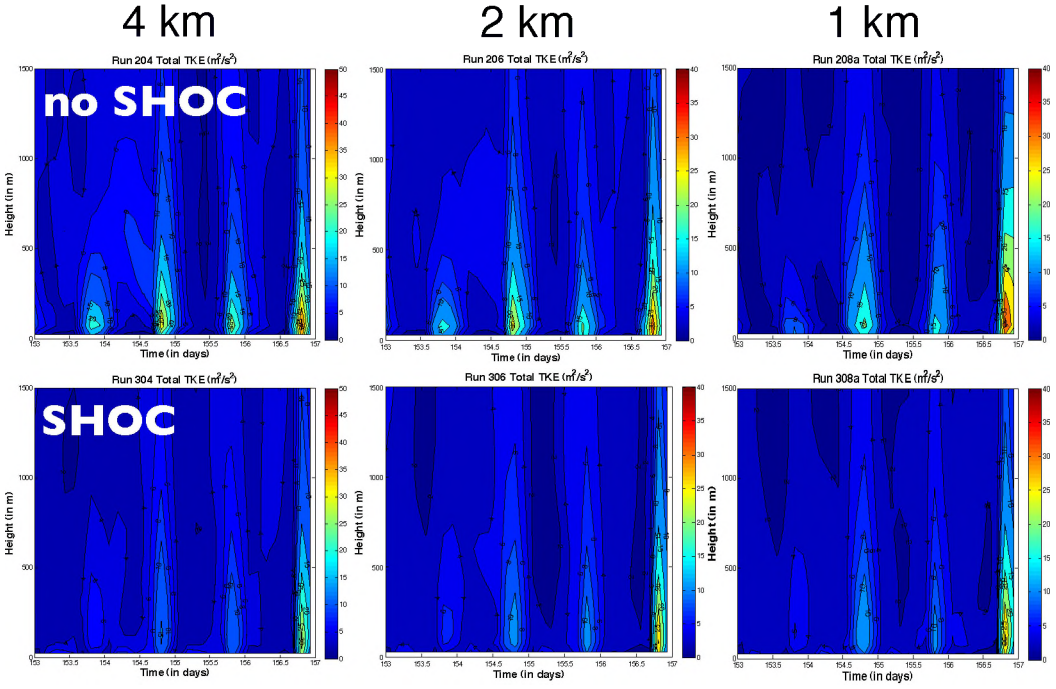

Figure 3: Simulated total (resolved plus subgrid-scale) turbulence kinetic energy during the fair-weather period with and without SHOC for horizontal grid sizes of 1, 2, and 4 km.

grid sizes (1, 2, and 4 km). The simulated deep convection exhibited unrealistically large maximum horizontal and vertical velocities, which suggests that the simulations need to be re-run with even smaller time steps. (Many simulations were already re-run with the time step halved.) The simulations that used SHOC generally had larger maximum velocities than identical simulations without SHOC.

We evaluated fair-weather and deep-convective boundary layer profiles in M3CE simulations. The simulated boundary layer profiles during a 4-day period with fair weather were unrealistically dry and cold for all horizontal grid sizes, while those during a 6-day period with deep convection were in good agreement with observations when using a 1-km grid size, but unrealistically dry and cold when using a 4-km grid size. There are several possible reasons for the disagreements during the fair-weather period that are being investigated. The subgrid-scale TKE profiles during the fair-weather period exhibit more realistic profiles when using SHOC, as expected. Simulations with SHOC exhibited grid size independence of total TKE, while those without SHOC did not (Fig. 3).

5. Tests against large-eddy simulations

At NCAR, Peter Bogenschutz and Chin-Hoh Moeng performed the first test of the Diagnostic Higher-Order Closure (DHOC) with SAM using a grid spacing of 1.6 km. The DHOC scheme has been slightly simplified and renamed to SHOC (Simple Higher-Order Closure). In order to verify the result, we simulated the same case (with the same initial setup, sounding, and external forcing) as the Giga-LES of a GATE tropical deep convection system. The radiation (RRTM) and microphysics (single-moment) schemes are also the same.

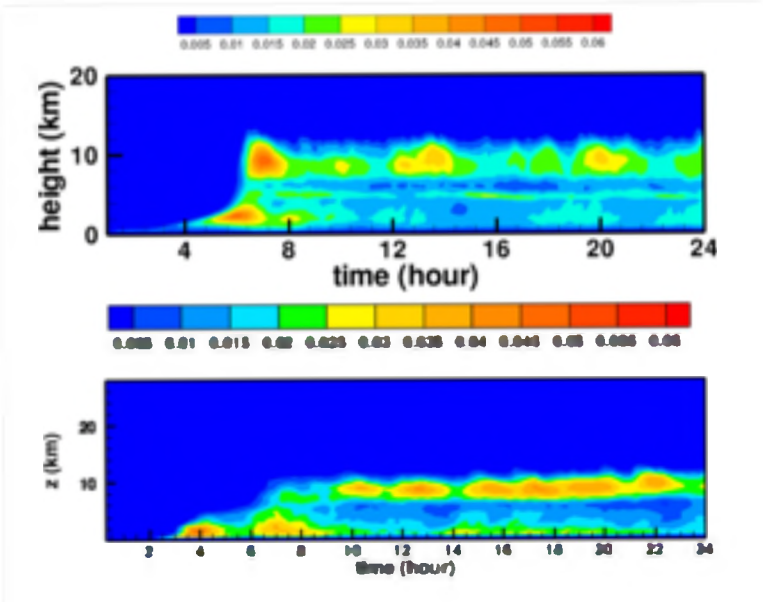

Fig.4: Comparison of the time evolution of the horizontally averaged cloud amount from Giga-LES (top panel) and from SAM using SHOC (bottom).

The time evolution of the horizontally averaged cloud amounts is compared in Fig. 4. Both simulations yield peak cloud amount at z ~ 9 km, but the CRM run failed to generate the mid-level congestus clouds and also produced too much low clouds.

Fig. 5 compares the vertical profiles of the horizontally averaged mass fluxes (by updrafts

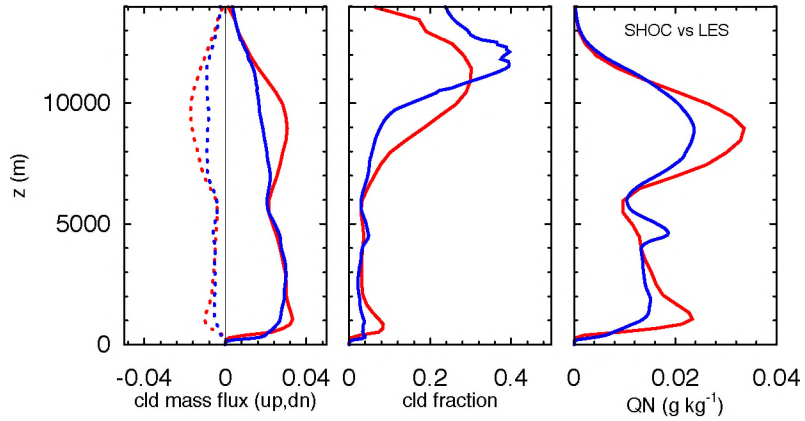

Fig. 5: Comparison of vertical distributions of the horizontally averaged mass fluxes (by updrafts and downdrafts, respectively), cloud fraction, and non-precipitating cloud amount. Blue curves are from the Giga-LES and red curves are from SAM using SHOC.

and downdrafts, respectively), cloud fraction, and non-precipitating cloud amount, all averaged over the last 12 hours of simulations. Using SHOC, SAM is able to produce reasonable horizontally averaged cloud field. But again the CRM failed to produce the mid-level clouds. It also overestimated the deep and shallow cloud amounts.

Figure 6 shows the vertical-velocity power spectra at two heights: 1 km and 5 km. SAM-

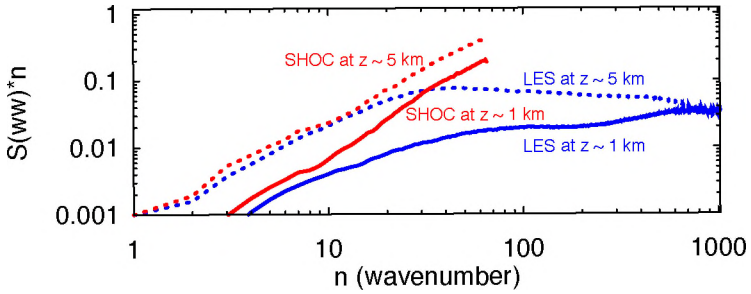

Fig. 6: Comparison of the vertical-velocity power spectra from Giga-LES (blue curves) and SAM using SHOC (red curves).

SHOC overestimated the vertical-velocity fluctuations near the grid scales, indicating further energy drainage to sub-grid scales is needed.

To further improve the CRM-SAM performance, we are now implementing a new SGS scheme (on top of the SHOC scheme) to include the "near-grid-scale" effect (i.e., effect from the largest SGS eddies).

We also plan to test SAM for two ARM cases (TWP-ICE and MC3E) against two new Giga-LESs when these benchmark simulations become available early next year.

6. Tests of SHOC in SP-CAM

SHOC has also been undergoing testing within the super-parameterized version of the Community Atmosphere Model (hereafter SP-CAM). The goal is to improve the representation of SGS processes, such as low-level clouds and turbulence associated with deep convection, with minimal computational increase. As an initial test we ran the baseline SP-CAM and SP-CAM-SHOC configurations for five-year integrations.

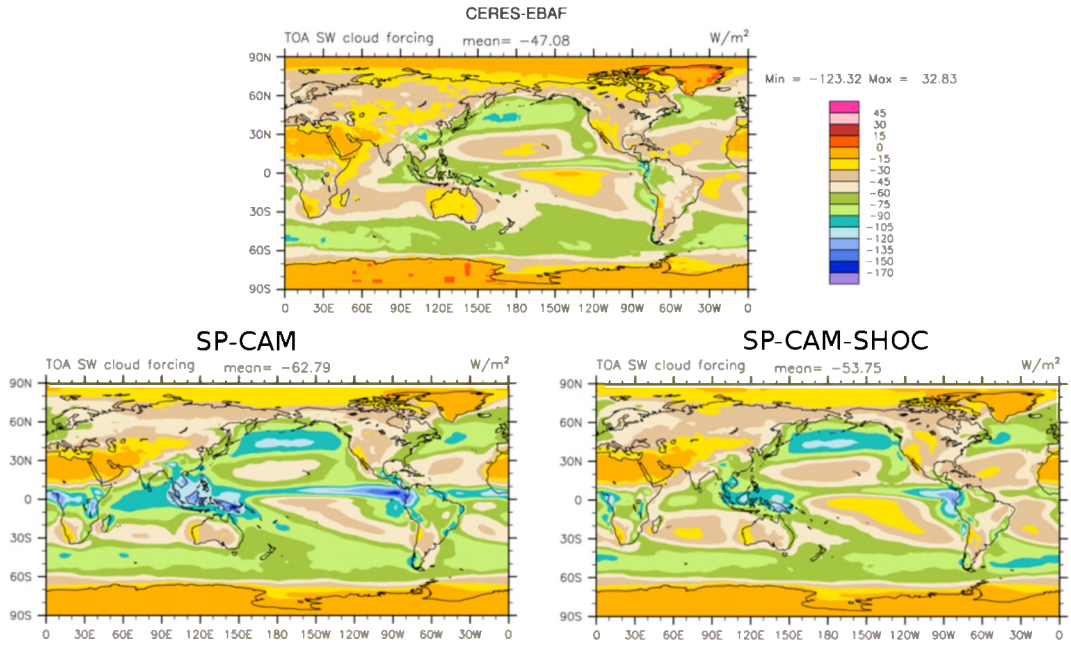

Fig. 7: Shortwave cloud forcing from observations (top row), SP-CAM (bottom left), and SP-CAM-SHOC (bottom right).

Figure 7 shows the annually averaged shortwave cloud forcing (SWCF) for CERES-EBAF observations and the two SP-CAM configurations. It is important to note that SP-CAM was never purposefully tuned to match observations, as many atmospheric general circulation models are. However, SP-CAM suffers from biases that cannot be ameliorated by simple tuning. An example can be found off the coast of Peru, where stratocumulus clouds are too dim (i.e. SWCF that is too weak) and further offshore where trade-wind cumulus clouds are too bright (i.e. SWCF that is too strong).

The annually averaged SWCF simulated by SP-CAM-SHOC shows ubiquitous improvements in the sub-tropics and tropics, relative to SP-CAM. The clearer distinction between stratocumulus and cumulus clouds in SP-CAM-SHOC simulations is arguably the most notable improvement. The two main reasons for the improved simulation is due to 1) more efficient SGS transports of heat and moisture in the embedded CRM and 2) consideration of SGS condensation. Similar to SP-CAM simulations, SP-CAM-SHOC has not yet been purposefully tuned to observations. In addition, SP-CAM-SHOC is only 30-35% more expensive than SP-CAM.

Future work will involve a detailed analysis of SP-CAM-SHOC simulations, for both the mean-state climate and tropical variability. In addition, the improvements shown for cloud forcing should translate to improved simulations in coupled runs. Thus, a preliminary coupled simulation of SP-CAM-SHOC has been started.

7. Work with CLUBB

UWM's role in the project is primarily to test CLUBB, one of the four PDF parameterizations involved in the project. In the past year, UWM focused on three tasks.

First, UWM has configured CLUBB to run the MC3E case of deep convection at the ARM-SGP site. UWM's initial conditions and forcings match those implemented in SAM by M. Khairoutdinov to simulate MC3E. Single-column simulations of the MC3E case have been performed using CLUBB. In these simulations, UWM has experimented with several configurations of CLUBB.

Second, UWM has been collaborating with PNNL to develop SAM_CLUBB, a version of SAM that uses CLUBB to parameterize small-scale clouds and turbulence. SAM_CLUBB has been used to successfully simulate the MC3E case.

Third, UWM has been assisting PNNL in the development and testing of SPCAM5_CLUBB, a version of SP_CAM5 that contains CLUBB.

PNNL collaboarated with Vincent Larson's group at the University of Wisconsin - Milwaukee on improving SAM_CLUBB simulations for deep convective clouds and SPCAM5 simulations with CLUBB. The PNNL focus has been on improving the coupling between cloud microphysics and CLUBB in SAM_CLUBB and SPCAM5_CLUBB. Here we summarize our progress in the past fiscal year.

For the SAM single-moment microphysics (sam1mom) in the default SAM_CLUBB configuration, total water (water vapor + liquid water) is used in CLUBB and saturation vapor pressure with respect to liquid water is used to diagnose cloud fraction in CLUBB. It may therefore under-predict cloud fraction from ice clouds. In the updated version, we have used the total water that includes both liquid water and ice water in CLUBB. What is more, a saturation vapor pressure that is the temperature-weighted mean of saturation vapor pressure with respect to liquid water and ice water is used to diagnose cloud fraction. The temperature-dependent formula used in the default SAM single-moment microphysics is still applied to partition total cloud condensate into liquid and ice condensate. Our SAM_CLUBB simulation with these updates now predicts surface precipitation rate and total precipitable water comparable to those from

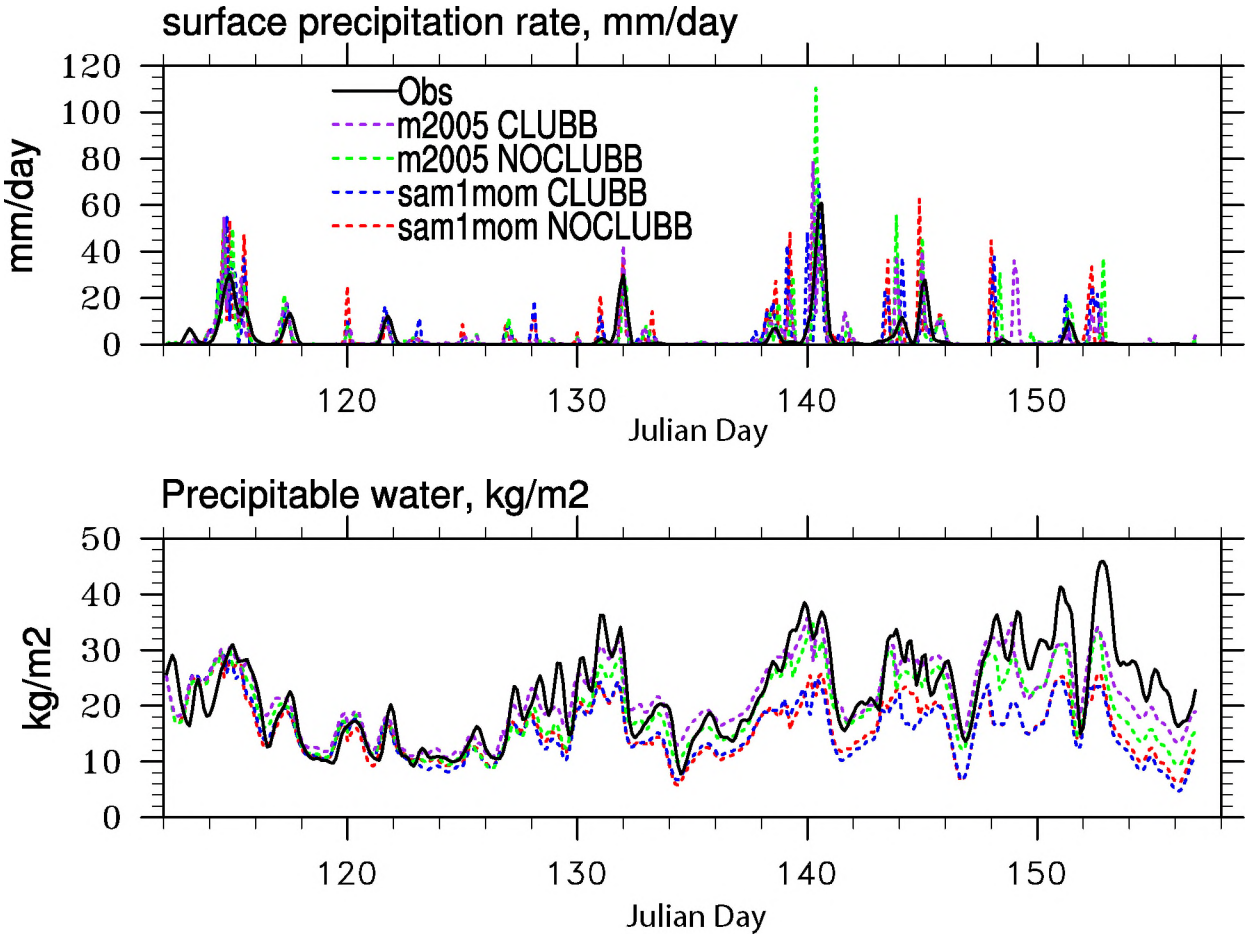

Figure 8: Time series of simulated (top) surface precipitation rate (mm/day) and (bottom) precipitable water (kg/m2) for the MC3E case of deep convection from SAM with four different configurations: one-moment microphysics without CLUBB (sam1mom NOCLUBB, red dashed line) and with CLUBB (sam1mom CLUBB, blue dash line); two-moment Morrison microphysics without CLUBB (m2005 NOCLUBB, green dash line) and with CLUBB (m2005 CLUBB, purple dash line). Observations are shown as solid black lines. The 2D version of SAM with 64 4-km CRM columns and 32 vertical layers is used.

SAM simulations without CLUBB (Fig. 8). These changes have also been incorporated into SPCAM5. The SPCAM_CLUBB results show reasonable global cloud fields (not shown), and

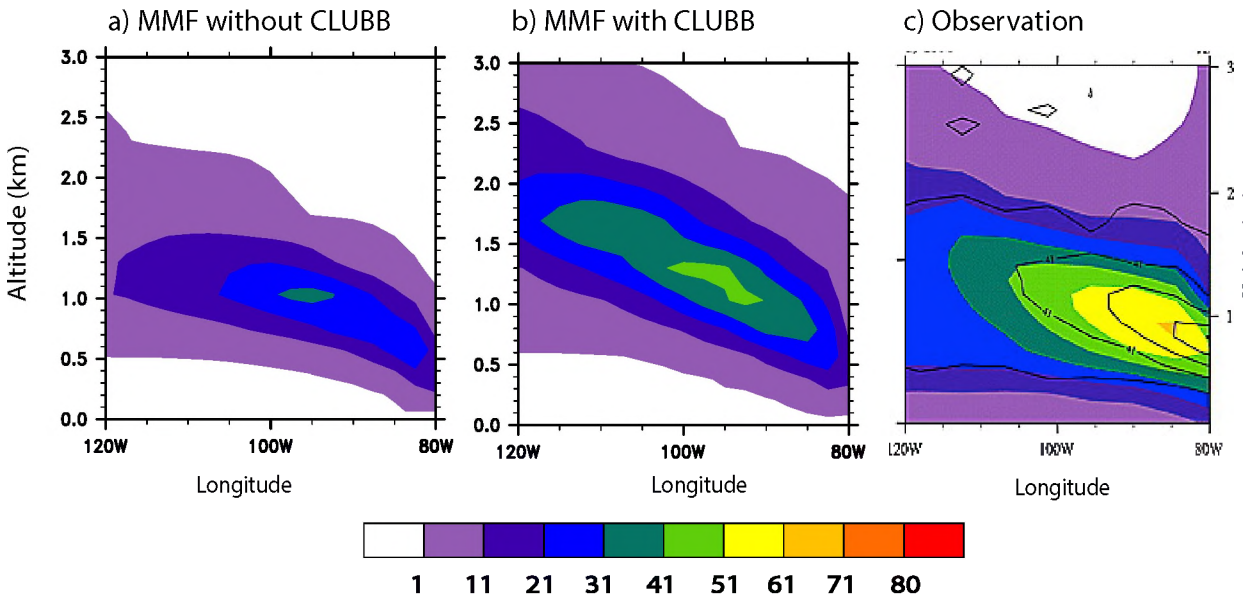

Figure 9: Cross-sectional plots of annual mean cloud fraction (%) along 15°S over the Southeast Pacific from a) SP-CAM with single-moment cloud microphysics scheme without CLUBB; b) SP-CAM with single-moment cloud microphysics scheme with CLUBB; c) C3M observations.

improved stratocumulus simulations (Fig. 9).

For the Morrison two-moment cloud microphysics (m2005) in the default SAM_CLUBB, liquid cloud fraction predicted in CLUBB is used to derive in-cloud cloud properties needed for the Morrison microphysics for those grid points with non-zero liquid cloud fraction. This can potentially overestimate in-cloud mixing ratios for hydrometers other than liquid water and thereby may lead to excessive depletion of these hydrometers. We have implemented a fractional cloudiness scheme into the Morrison microphysics scheme to handle the fractional cloudiness predicted by CLUBB. What is more, the ice cloud fraction formula from CAM5 is used to predict ice cloud fraction in SAM_CLUBB. The SAM_CLUBB results with the fractional cloudiness shows that SAM_CLUBB produces precipitable water comparable or better than that from SAM without CLUBB (Fig. 8). We are currently working on using the aforementioned fractional cloudiness scheme to couple the Morrison microphysics and CLUBB in SPCAM5.

8. IPHOC

Anning Cheng has made considerable progress since last October. The deliverables for these tasks include testing of the intermediately-prognostic higher-order turbulence closure (IPHOC) in the System for Atmospheric Modeling (SAM), in the Community Atmosphere Model version 5 (CAM5), and in the SP-CAM. The first task is full supported by this funding and will be presented in detail below, while the other two tasks are partially supported and will be presented briefly.

A) Results from implementing and testing IPHOC in SAM

The CRM used in this study is version 6.10.3 of SAM. The unmodified (control) version of the model has a 1.5-order turbulence closure with prognostic turbulence kinetic energy (TKE). In order to study the influence of turbulence on the simulation of mesoscale convective systems during MC3E, the IPHOC scheme is implemented in the SAM, and referred to as the SAM-IPHOC.

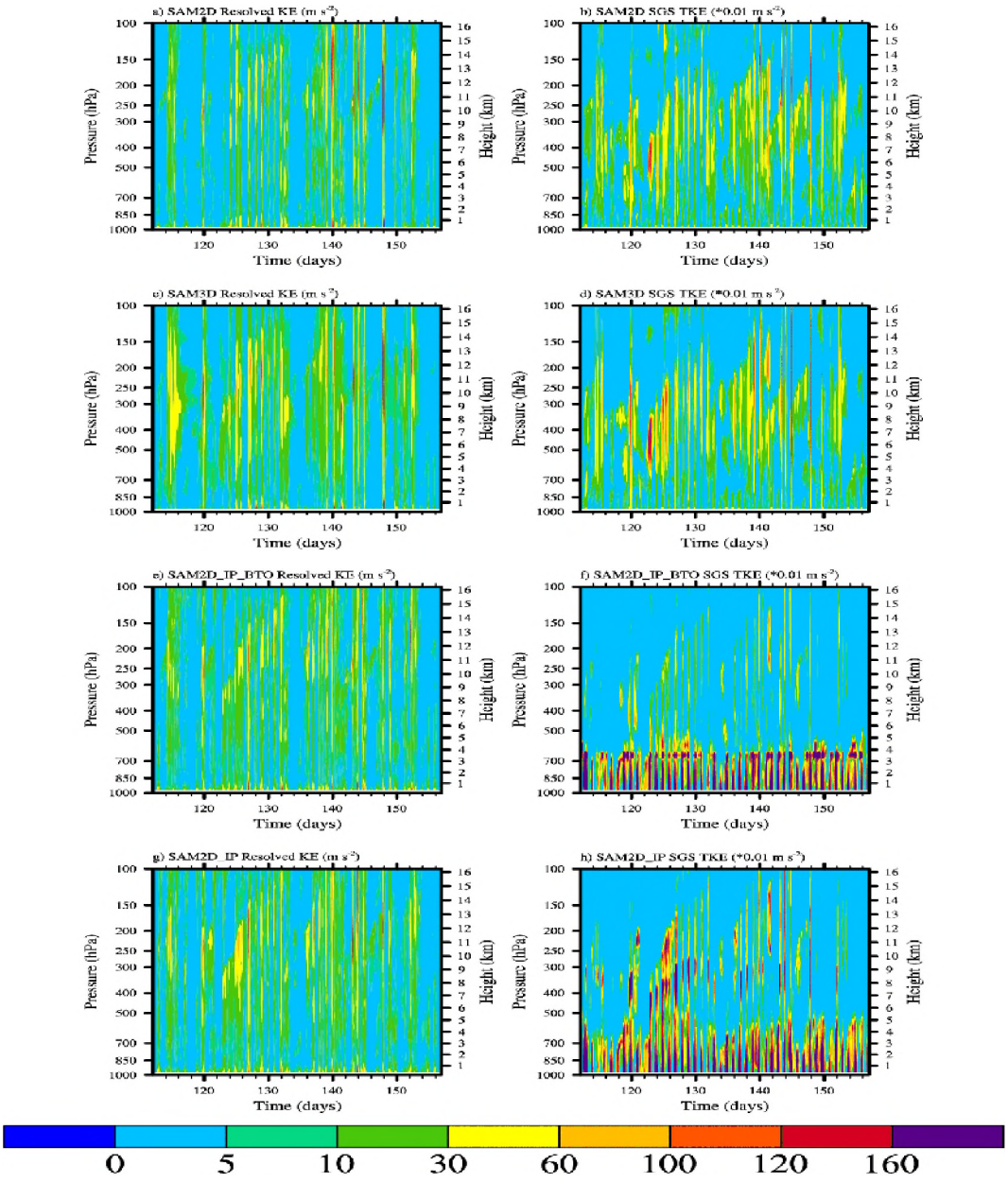

Figure 10. Time evolution of the resolved kinetic energy (KE) from SAM2d (left column) (a), SAM3D (b), SAM2D-IP-BTO (c), and SAM2D-IP (g); and subgrid-scale (SGS) turbulence kinetic energy (TKE) from SAM2d (right column) (b), SAM3D (d), SAM2D- IP-BTO (f), and SAM2D-IP (h).

Four experiments (numbered 1 through 4 below) were run for 45 days beginning on day 112 to cover the entire MC3E period: 1) a two dimensional SAM with the 1.5- order turbulence closure (labeled as SAM2D) was run with a horizontal domain of 256 km and a grid-size of 4 km; 2) a three dimensional SAM with the 1.5-order turbulence closure (labeled as SAM3D) was run with a horizontal domain of 64 km x 64 km and a grid-size of 4 km to explore the influence of the dimensionality; 3) same as experiment one except with the IPHOC scheme activated in the lowest 3 km (labeled as SAM-IP- BTO) performed to investigate the effects of turbulence in the boundary layer; and 4) same as experiment one except with the IPHOC scheme activated in the entire vertical column (labeled as SAM-IP). The effects of the turbulence in the free troposphere on the simulation of the mesoscale convective systems can be explored by comparing SAM-IP and SAM-IP-BTO. The vertical grid-spacing for all experiments are 50 m near the surface and stretch to 1 km at the model top (27 km).

Although the subgrid-scale (SGS) TKE is about two-orders of magnitude less than the resolved KE (Figure 10), the differences of the SGS TKE between the 1.5-order closure and the IPHOC is much larger than those of the resolved KE. The SGS TKE from the IPHOC is substantially larger than from the 1.5-order turbulence closure for both the boundary-layer and free troposphere (Figures 10b, 10d, 10f, and 10h). This may be due to efficient buoyancy production and nonlocal transport. IPHOC also produces much stronger turbulence and larger SGS-TKE above the boundary-layer than the 1.5-order turbulence closure (Figures 10f and 10h). It is interesting that the effect of the dimensionality is similar to the SGS schemes since the SGS-TKE from the SAM3D is also larger than from SAM2D, examples of this effect are apparent for day 120, 124, and 125.

The resolved KE from the simulations with the IPHOC scheme is generally larger and its duration from the cloud evolution of convective episodes lasts longer than that from simulations with the 1.5-order closure. An example is the convective episode between day 124 and day 128. The SAM2D-IP produces the largest resolved KE and its duration is the longest among all the experiments. The impacts of the SGS TKE on deep convective clouds are likely different from its viscosity effects on boundary-layer clouds. Cheng and Xu [2008] found that the resolved KE tends to decrease when the SGS TKE increases and the higher-order turbulence SGS model absorbs the additional SGS TKE for boundary-layer clouds. In addition to the viscosity effects, the SGS TKE may enhance the cloud condensation processes inside clouds and latent heat release, thus promoting the circulation of the mesoscale convection. The enhancing effects of the cloud processes by the SGS TKE may be more important in MC3E.

The dimensionality on the resolved KE is similar to the effects of the SGS TKE. One possible reason is that the SAM3D produces larger SGS TKE than SAM2D. 3-D circulation may be a contributing factor as well. For example, the resolved KE from SAM3D between day 102 and day 104 is the strongest, and the episode lasts the longest among all experiments. However, different entrainment, detrainment, and energy dissipation between 2D and 3D are profound and beyond the scope of this report.

The resolved KE and SGS TKE are not easily calibrated because no observations exist. The total precipitable water and surface precipitation from the simulations with different SGS schemes, on the other hand, can be compared with observations and the SGS scheme can be justified indirectly. The total precipitable water from the SAM2D-IP compares most favorably with MC3E observations among all experiments. The SAM2D and SAM3D seriously

underestimate the precipitable water after day 135. The SAM2D- IP-BTO experiment with the IPHOC only below 3 km still underestimates precipitable water, but performs better than the SAM2D or SAM3D. One possible reason is because SAM2D-IP and SAM2D-IP-BTO produce less precipitation between day 124 and day 130 than the other two experiments.

The importance of the turbulence above 3 km is obvious by comparing the results from

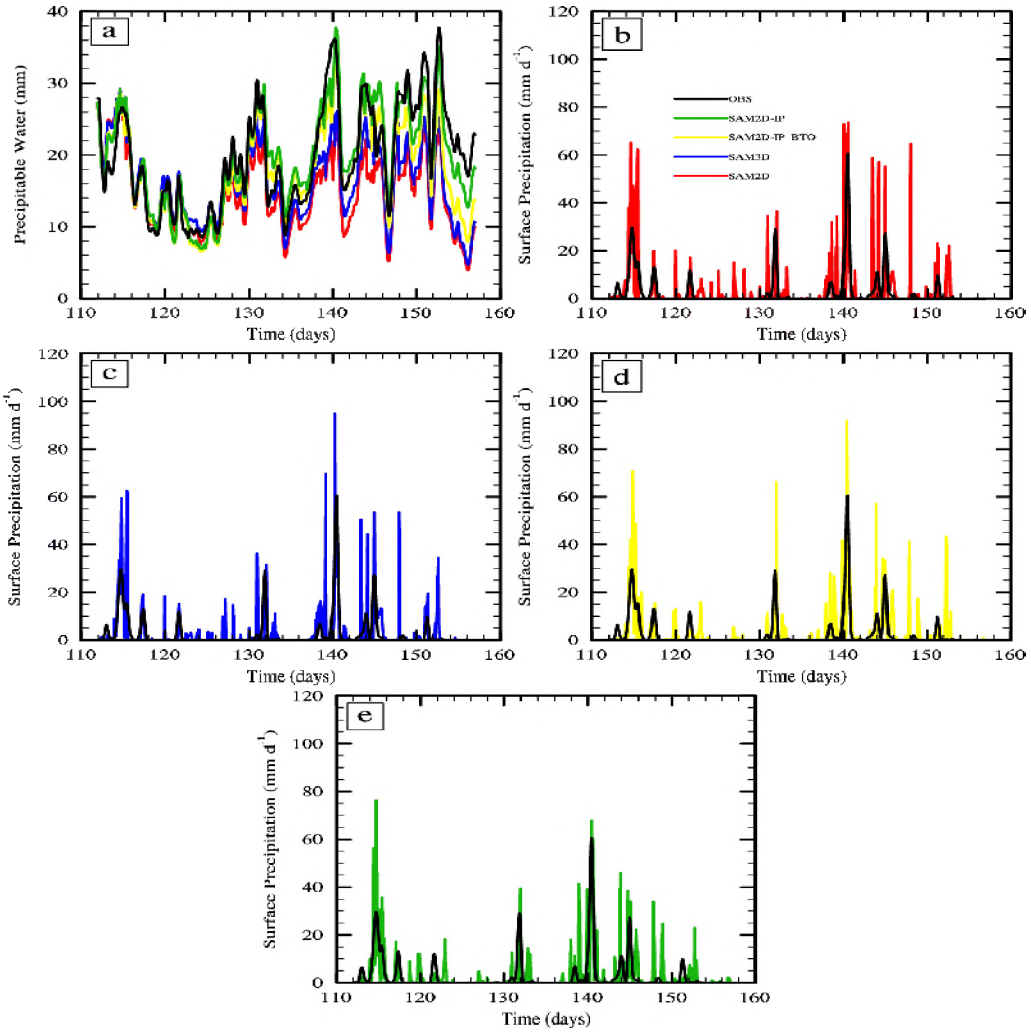

Figure 11. Time series of precipitable water (a, mm) from SAM2d (red), SAM3D (blue), SAM2D-IP-BTO (yellow), SAM2D-IP (green), and observation (black); time series of surface precipitation rate (mm/day) from SAM2D and observation (b), from SAM3D and observation (c), from SAM2D-IP-BTO and observation (d), and from SAM2D-IP and observation (e).

SAM-IP and SAM-IP-BTO (Figure 11a, 11d, and 11e). SAM-IP-BTO underestimates precipitable water and produces more precipitation after day 135 than both SAM-IP and MC3E observations. The sustainable and strongly resolved circulation shown in Fig. 10 may part of the reason and will be investigated in an upcoming paper [Cheng and Xu, 2013d].

B) Preliminary Results from Implementing IPHOC in CAM5

The implementation and testing of IPHOC in CAM5 is ongoing. Preliminary results indicate that the CAM5 with IPHOC is able to produce more reasonable low-level clouds, liquid water content, and cloud regime transition than CAM5.

The simplified and optimized IPHOC is implemented in CAM5 (hereafter CAM5- IP) supported by ASR SC0005450 and SC0008779. The IPHOC replaces the planetary boundary-layer (PBL), shallow convection, and cloud macrophysics parameterizations in CAM5. The CAM5-IP represents a more unified treatment of boundary layer and shallow convective processes.

We used CAM3.5 with a 2D CRM embedded in each of its atmospheric grid columns. The CRM is the System for Atmospheric Modeling (SAM) with the IPHOC scheme implemented. This model is hereafter referred to as SPCAM-IPHOC, and the model without IPHOC is called SPCAM.

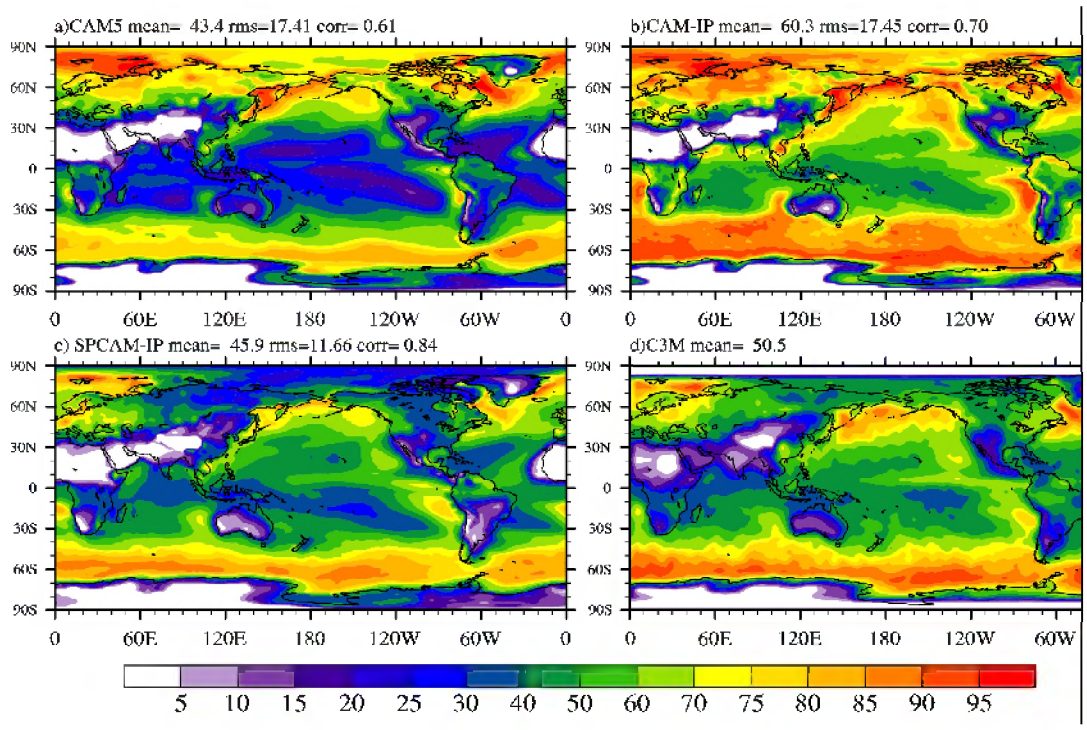

Figure 12. Global distribution of boreal winter (December, January, and February) mean low-level (below 700 hPa) cloud amounts (%) from CAM5 (a), CAM5-IP (b), SPCAM- IPHOC (c), and C3M observations (d).

Three sets of experiments were performed: 1) a ten year and three-month simulation using CAM5 with a finite-volume (fv-) 1.9°X2.5° dynamic core starting from September 1, 1997; 2) Same as 1) except using CAM5-IPHOC and integrating the model for 1 year; and 3) Same as 1) except using the SPCAM-IPHOC with two more vertical levels for lower atmospheric levels ($p > 700$ hPa) compared with set 1 to better resolve boundary-layer clouds. The results from the winter of the first year are used in this study.

Much improvement can be seen in the cloud amount and location of low-level clouds simulated by the CAM5-IPHOC (Fig. 12). Both CAM5 and SPCAM-IPHOC underestimate global mean low-level clouds. The extent, strength and location of the low-loud maxima in the northeastern (NE) Pacific, the southeastern (SE) Pacific, and SE Indian ocean (west coast of Australia), were better reproduced by CAM5-IPHOC, while those from CAM5 are either too weak or do not cover an area as large as observations, e.g., the SE Indian ocean in CAM5, as shown in Figure 12a. The global annual-mean low- cloud amount from the CAM5-IPHOC-hires is 60.3%, which compares to 50.5% from merged CloudSat, CALIPSO, CERES and MODIS (C3M) observations from January 2007 through December 2008. The global mean from CAM5 is 43.4%, which is less than C3M observations. The vertical structure of the boundary-layer clouds is also improved in CAM5-IPHOC (Figure 12). The pattern of the cloud structures from CAM5-IP, represented by the cloud fraction and cloud water content in the vertical cross section along 15°S in the Southern Pacific, compares well with the C3M observations. The shallow cumulus clouds from CAM5 are shallower and have less liquid (not shown), while those from SPCAM-IPHOC are deeper and have more liquid than from C3M observations.

C) Results from an Upgraded SP-CAM with IPHOC in its CRM component

The analysis of output from the 10 year and 3 month simulations with SPCAM- IPHOC, and several short-term sensitivity experiments are documented results in a series of papers (Cheng and Xu 2013a, b; Xu and Cheng 2013a, b;). Cheng and Xu (2013a) examined the seasonal-mean cloud regime transitions along a transect from the subtropical California coast to the tropics for the June, July, and August (JJA) season, and compared to CAM5, SPCAM and SPCAM-IPHOC results. A primary conclusion of this study is that there are qualitative agreements in the characteristics of cloud regimes along the transect between the models, with SPCAM-IPHOC producing the most realistic cloud-regime transition. Cheng and Xu (2013b) provided a detailed analysis of austral-spring stratocumulus clouds in the southeastern (SE) Pacific and discussed physical mechanisms of the diurnal variation. The SPCAM-IPHOC simulation can reproduce the spatial pattern of the diurnal variations of low clouds within the SE Pacific region. The maximum cloudiness and liquid water path occur in the early morning and the minimum occurs in the late afternoon over open ocean. Two diurnal variation mechanisms have been examined in this study. The diurnal variations in large-scale circulations include the poorly resolved, orographically induced land-sea circulations in SP-CAM, in particular, the upsidence wave, which impacts diurnal variation near the coast. The solar-forced variation dominates the diurnal variation over the open ocean, as expected.

Xu and Cheng (2013a) showed that the SPCAM-IPHOC model can produce global- and annual-mean low cloud amounts that are within 5.3% of observations from C3M (Kato et al. 2011). The spatial distributions of low clouds are realistic for several ocean basins, with the relationship of low clouds with large-scale variables agreeing with those observed in these ocean basins. Xu and Cheng (2013b) showed that the seasonal variations of these low-level clouds in the eastern Pacific are comparable to and, in some instances, better than those produced by the best regional high-resolution climate models (Wyant et al. 2010; Wang et al. 2011). The spatial distribution and seasonal variation of several variables agree with available satellite observations.

9. A Mini-LES

During the reported period, Marat Khairoutdinov has been working on improving the super- parameterized CAM (SP-CAM) model to better represent shallow clouds and pbl turbulence. Those have been long-standing deficiencies of the first generation of SP-CAM. The main reason for that is rather coarse horizontal grid spacing (typically 4 km) of the cloud-resolving model used as the super- parameterization. Such a resolution has been demonstrated to work reasonably well to represent large deep clouds; however, it has been generally agreed that it is not adequate to represent relatively small shallow clouds. Those clouds are among the main reasons of uncertainty in climate change projections of the GCMs. Even the sign of the shallow-cloud feedback on the shortwave forcing is currently quite uncertain.

One of the ways is to implement some high-order closure parameterization of shallow clouds. This is the area where other researchers of this project are working on. As the original developer of the SP-CAM, Marat believes in avoiding parameterizations in the first place. Instead, he is testing incorporation of a second super-parameterization, specifically for shallow clouds, to work in tandem with the deep-cloud super-parameterization. Note that a simple increase of the horizontal resolution of the SP, say to 400 m, would increase the expense of the already very expensive SP-CAM by two orders of magnitude.

The idea is to use a small-domain 2D CRM with high-horizontal resolution if 250m, and the same number of columns as the SP, that is 32. To distinguish such a model from the SP, it was terms "Mini-LES". To avoid deep convection in such a small domain, the condensation above 5000 m is artificially suppressed. The mini-LES is forced by the large-scale tendencies of the climate model as the SP. The SP is called after the Mini-LES. To avoid double counting of the vertical fluxes, the vertical mini-LES fluxes are subtracted from the sub-grid scale fluxes of the SP. The Mini-LES supplies the cloud water and cloud fraction information to the radiation computations on the SP grid. The preliminary results are encouraging. The MiniLES seems to improve low cloud distribution in short climate simulations. Still there are problems with the technique that are currently being worked on. Also, we plan more tests using single- column approach. We also will compare the results with the SP-CAM versions with other SGS parameterizations developed by other groups of this project.

10. Further tests of SHOC

We have successfully implemented SHOC into the Colorado State University (CSU) MMF. The CSU MMF represents a coupling between NCAR's Community Atmosphere Model (CAM) and the System for Atmosphere Modeling (SAM; Khairoutdinov and Randall 2003) cloud resolving model (CRM). Thus, the CSU MMF is known as the "superparameterized" CAM (SP-CAM; Khairoutdinov et al. 2005). Here we implemented SHOC into SAM, to replace the simple 1.5 TKE closure with an assumed-PDF based parameterization.

SP-CAM-SHOC has been successfully run for multi-year climate simulations for two configurations; one with the default single-moment microphysics scheme and one using the Pacific Northwest National Laboratory (PNNL) configuration, which uses a double moment microphysics scheme and sophisticated aerosol treatment. In both configurations, SP-CAM-SHOC improves the realism of the simulations compared to the default SP-CAM.

Figure 13 shows the shortwave cloud forcing biases, computed relative to CERES- EBAF, for SP-CAM (left column) and SP-CAM-SHOC (right column) run with both the simple

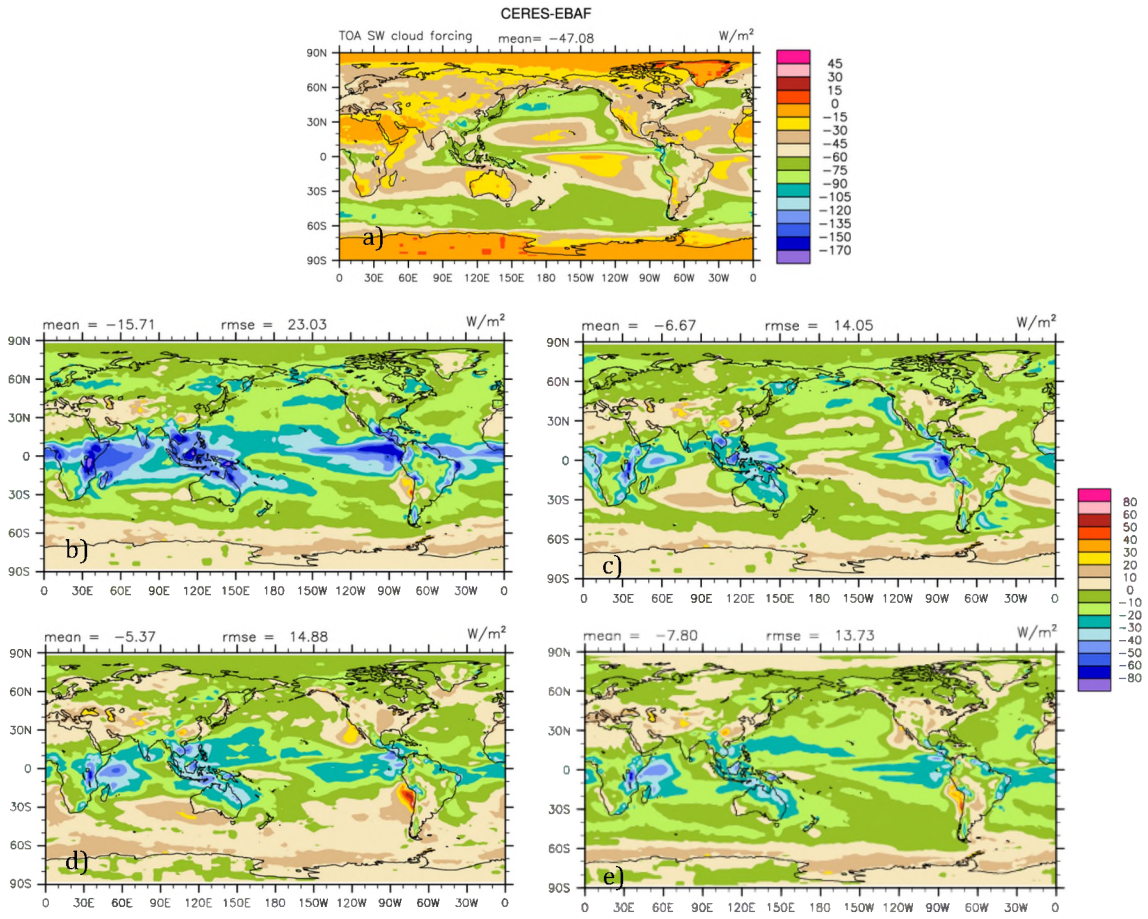

Figure 13: Shortwave cloud forcing from a) CERES-EBAF observations (top), and the shortwave cloud forcing biases computed relative to CERES−EBAF for b) SP−CAM, c) SP−CAM−SHOC, d) PNNL−SP−CAM, and e) PNNL−SP−CAM−SHOC.

microphysics (middle row) and the PNNL configuration (bottom row). Cool colors indicate regions where the simulated clouds are too reflective and warm colors indicated regions where the simulated clouds are not reflective enough. It is clear that for both the single and double microphysics cases that SP-CAM-SHOC improves the overall RMSE score, compared to the standard SP-CAM. However, more importantly, SP-CAM-SHOC ameliorates several regional biases present in SP- CAM.

Since the embedded cloud resolving model in SP-CAM has a horizontal grid size of 4 km, low-level boundary layer clouds, such as stratocumulus (Sc) and cumulus (Cu) are not resolved. In addition, the simple 1.5 TKE closure and “all or nothing” condensation scheme in SP-CAM are inadequate to properly parameterize these types of clouds. This is evident in Figure 1 for SP-CAM simulations, which generally shows a lack of Sc clouds off the western coasts of the continents (more specifically, the Peruvian and Californian Sc regions). SP-CAM-SHOC, with its

better treatment of SGS turbulence and clouds, greatly improves the representation of maritime Sc clouds.

In addition, the improved representation of maritime Sc in SP-CAM-SHOC is not at the expense of the simulated climate. As demonstrated in Figure 13, improvements in the simulated shortwave cloud forcing can also be seen in the tropics. This is related to improved representation of SGS mixing in SHOC, which prevents deep convection from being too intense (Varble et al. 2011). While not shown, SP-CAM- SHOC also marginally improves other aspects of the climate simulation such as precipitation and surface temperature. The overall "Talyor score", a metric that gives the quality of a climate simulation in one objective number, is better for SP- CAM-SHOC than SP-CAM. Results of these climate simulations are described in a peer-reviewed paper to be submitted soon.

1a) Aerosol-Cloud Interaction Experiments with SP-CAM-SHOC

It is widely agreed that most conventionally parameterized GCMs overestimate the positive relationship between aerosol optical depth and liquid water path (Quass et al. 2009), resulting in large changes in the cloud radiative effects. This can result in an unrealistic simulation of the 20th century, as well as misleading climate change simulations. Wang et al. (2011) showed that the PNNL SP-CAM greatly reduces the indirect effects due to aerosols, compared to conventional GCMs, because precipitation processes were shifted primarily from autoconversion to accretion, due to a prognostic precipitation scheme. However, the PNNL SP-CAM does not realistically simulate low-level clouds, in which aerosol effects can be potentially very climatically important.

We ran the PNNL SP−CAM with SHOC with present day and pre-industrial aerosol emissions to asses the aerosol-cloud interactions when low level clouds and turbulence are better represented. Simulations are five years in length. Table 1 presents the changes in top of atmosphere flux perturbations, the aerosol-cloud radiative effects, and the changes in liquid water

Simulation	ΔR (W/m2)	ΔCRE (W/m2	ΔSWCF (W/m2)	ΔLWCF (W/m2)	ΔLWP (%)
SP-CAM (Wang et al. 2011)	-1.05	-0.83	-0.77	-0.06	+3.9%
SP-CAM-SHOC	-0.98	-0.62	-0.63	+0.01	+2.8%
CAM5-MG1 (diagnostic precipitation)	-1.50	-1.42	-1.79	+0.37	+8.9%
CAM5-MG2 (prognostic precipitation)	-1.08	-0.76	-0.91	+0.15	+5.8%

Table 1: Radiative flux perturbation from various simulations (all are five year simulations at 2-degree horizontal resolution). Differences shown are for simulation with 1850 and 2000 aerosol emissions. R = top of atmosphere flux, CRE = total cloud radiative forcing, SWCF = shortwave cloud forcing, LWCF = longwave cloud forcing, LWP = liquid water path.

path. Overall, SP-CAM-SHOC exhibits a slightly lower sensitivity to aerosols when compared to SP-CAM and a version of CAM5 that employees a prognostic precipitation scheme. The values SP- CAM-SHOC produces are well within the range of observational uncertainty (Quass et al. 2009).

1b) Coupled Experiments with SP-CAM SHOC

We recognize the importance of running coupled experiments with proposed parameterizations to detect any unwanted feedbacks that may inadvertently develop from improving a physical process. Thus, we ran the versions of SP-CAM and SP-CAM-SHOC with the simple single-moment microphysics scheme for 10 years in a pre-industrial control run configuration. Neither SP-CAM simulation was tuned to achieve a pre-industrial top of atmosphere radiation balance of ~0 W/m2, thus after 10 years of integration SP-CAM had an imbalance of 1.9 W/m2 while SP- CAM-SHOC had an imbalance of -1.4 Wm^{-2}.

Therefore, the simulations were stopped after 10 years as the climate would inevitiably drift with a longer integration. While both SP-CAM and SP-CAM-SHOC would need to be tuned before science could be performed in a coupled climate simulation, it is encouraging to note that there were no "surprises" from the SP-CAM-SHOC coupled simulation and that the improvements seen in the prescribed SST simulations (i.e. improved Sc) were also present in the coupled simulation. Therefore, we have high confidence that a tuned version of SP-CAM-SHOC will produce a successful climate simulation. Future work will focus on tuning the coupled simulation.

11. Testing SHOC on Deep Convective Regimes

In addition to testing SHOC in the SP-CAM framework, we simulated deep convective cases in the context of the standalone cloud resolving model, SAM. Here we used the ARM Tropical Warm Pool International Cloud Experiment (TWP-ICE) case.

Bogenschutz and Krueger (2013) had previously found that SAM-SHOC was less sensitive to changes in horizontal and vertical resolution for boundary layer clouds than the standard SAM with it's 1.5 TKE closure (hereafter referred to as SAM-TKE). Here we wish to examine the sensitivity of SAM-SHOC to changes in horizontal resolution for a deep convective case.

The ARM TWP-ICE case was simulated and compared between 1) LES using 2048 x 2048 x 256 grid points with a horizontal grid mesh of 100 m (often referred to as a GigaLES, performed at CSU by Don Dazlich and David Randall) and 2) SAM-TKE and SAM-SHOC with horizontal grid sizes of 0.8, 1.6, 3.2, and 6.4 km to test the scale sensitivity.

Figure 14 shows the temporally and spatially averaged profiles of total cloud condensate, total heat flux, and SGS heat flux from TWP-ICE simulations from day 19.75 to 20.5 (an active period) for both SAM-TKE and SAM-SHOC for grid sizes ranging from dx = dy = 0.8 km to 6.4 km. For the base case of dx = dy = 1.6 km, both SAM-TKE and SAM-SHOC show realistic simulation of deep convection with a distinct tri-modal distribution of clouds. Although not shown, an examination of the time evolution of the horizontally averaged cloud water and ice shows very similar and realistic behavior between these two configurations when dx = dy = 1.6 km. However, we wish to examine how robust the simulations are to changes in resolution.

Total condensate profiles shows an obvious sensitivity for SAM-TKE in simulating low-level clouds, while SAM-SHOC is much more robust. This result is not so surprising as SHOC was originally designed to treat unresolved low-level boundary layer clouds. However, it is also evident that SAM-SHOC shows sensitivity to the grid size for high-level clouds. The reason for this is currently not known but is being investigated. We are examining the coupling of SHOC with the ice microphysics as a potential culprit.

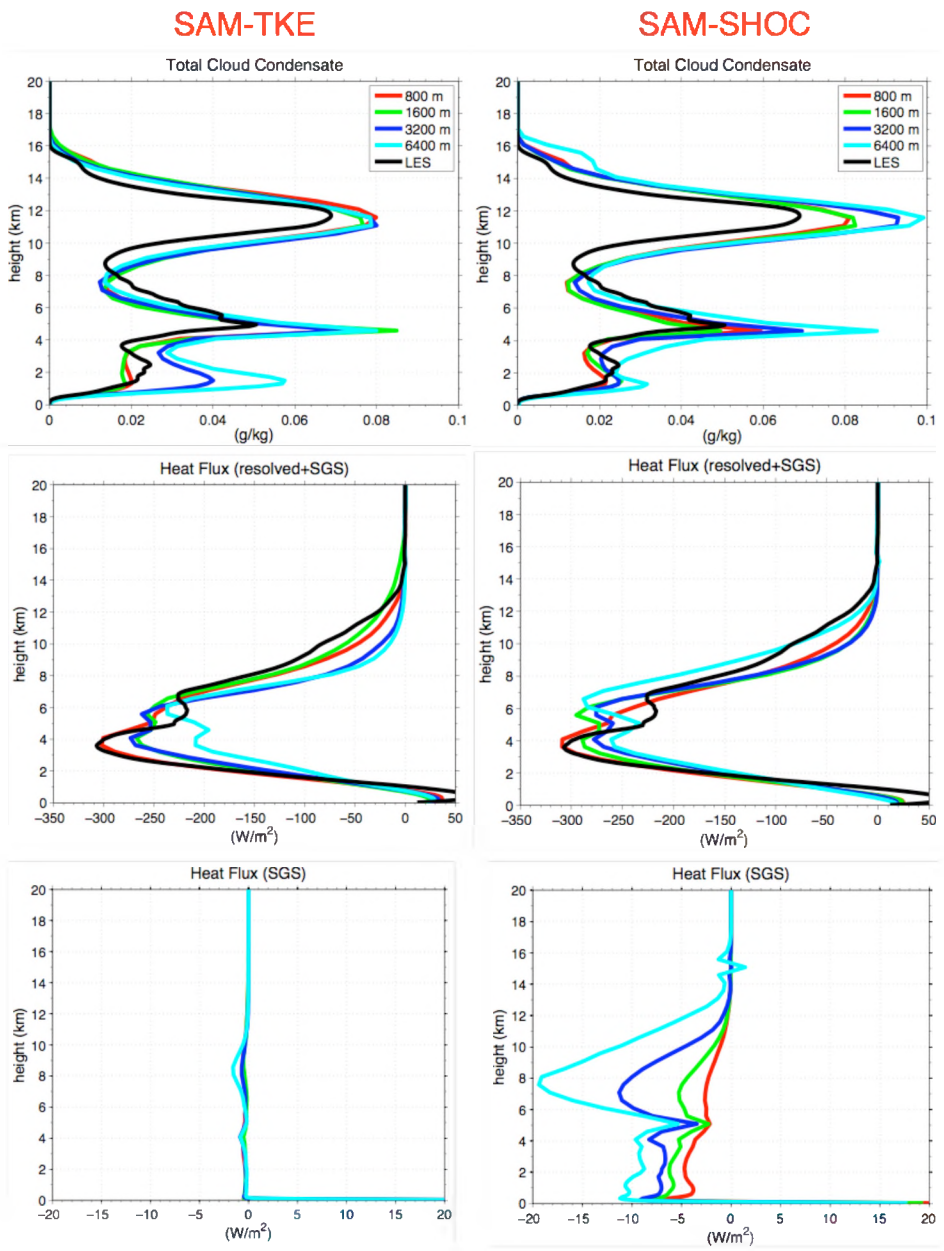

Figure 14. Temporally and spatially averaged profiles from TWP-ICE simulations from day 19.75 to 20.5 (active period) for (left) SAM-TKE and (right) SAM-SHOC for various horizontal grid sizes. The black curve represents the GigaLES.

An explanation of the sensitivities seen in the low-level clouds for SAM-TKE can be achieved by looking at the profiles for the heat flux. The horizontally and temporally averaged total heat flux profiles differ by 100 W/m2 between the SAM- TKE simulations at the coarsest and finest resolution. While SAM-SHOC also shows some sensitivity for the total heat flux, the differences are much smaller than those of SAM-TKE. A clearer picture emerges when only the SGS contribution is analyzed.

We would expect that as grid size increases, the simulated SGS contribution would increase, while the total heat flux remains the same. However, SAM-TKE has a negligible contribution to the SGS heat flux for all grid resolutions, suggesting an unrealistic partitioning between SGS and resolved heat flux. SAM-SHOC, however, does increase the SGS contribution as grid size increases. While this realistic partitioning behavior is encouraging, it should be noted that when a filter is applied to the GigaLES to determine the magnitude of the SGS heat flux for a particular grid size, it is obvious that SAM-SHOC is still underestimating the SGS turbulence for all grid sizes. Thus, future work will focus on improving SAM-SHOC's representation of SGS turbulence and heat fluxes for deep convection, for a more scale insensitive simulation.

References

Bogenschutz, P.A. and S. K. Krueger, 2013: A simplified PDF parameterization of subgrid-scale clouds and turbulence for cloud-resolving models. *J. Adv. Model. Earth Syst.*, **5**, 195-211.

Gettelman, A., H. Morrison, S. Santos, P. A. Bogenschutz, and P. M. Caldwell, 2014. Advanced two-moment bulk microphysics for global models. Part II: Global model solutions and aerosol-cloud interactions, *J. Climate*, **28**, 1288-1307.

Khairoutdinov, M. F., and D. A. Randall, 2003: Cloud-resolving modeling of the ARM summer 1997 IOP: Model formulation, results, and uncertainties, and sensitivities. *J. Atmos. Sci.*, **60**, 607-625.

Khairoutdinov, M. F., D. A. Randall, and C. DeMotte, 2005: Simulations of the atmospheric general circulation using a cloud-resolving model as a super- parameterization of physical processes. *J. Atmos. Sci.*, **62**, 2136-2154.

Quaas, J., and co-authors, 2009: Aerosol indirect effects – general circulation model intercomparison and evaluation with satellite data. *Atmos. Chem. Phys.*, **9**, 8697- 8717.

Varble, A., and co-authors, 2011: Evaluation of cloud-resolving model intercomparison simulations using TWP-ICE observations: Precipitation and cloud structure. *J. Geophys. Res*, **116**, D12.

Wang, M., S. Ghan, M. Ovchinnikov, X. Liu, R. Easter, E. Kassianov, Y. Qian, H. Morrison, 2011. Aerosol indirect effects in a multi-scale aerosol-climate model PNNL-MMF. *Atmos. Chem. Phys.*, **11**, 3399-3459.

Publications and Presentations Supported by This Project

Journal Articles:

Bogenschutz, P. A., 2015: Improving cloud and turbulence processes in cloud resolving GCMs. In preparation for *J. Adv. Model. Earth. Syst.* (to be submitted Dec. 2015).

Bogenschutz, P. A., A. Gettelman, H. Morrison, V. E. Larson, C. Craig, and D. P. Schannen, 2013. Higher-order turbulence closure and it's impact on climate simulations in the Community Atmosphere Model. *J. Climate*, **26**, 9655-9676, doi:10.1175/JCLI-D-13-00075.1.

Cheng, A., and K.-M. Xu, 2011: Improved low-cloud simulation from a multiscale modeling framework with a third-order turbulence closure in its cloud-resolving model component. *J. Geophys. Res.*, **116**, 19 pp. doi:10.1029/2010JD015362.

Cheng, A., and K.-M. Xu, 2013: Diurnal Variability of Low Clouds in the Southeast Pacific Simulated by a Multiscale Modeling Framework Model. *J. Geophys. Res.*, **118**, 9191-9208, doi:10.1002/jgrd.50683.

Cheng, A., and K.-M. Xu, 2013: Evaluating low-cloud simulation with an upgraded multiscale modeling framework model. Part III: Tropical and Subtropical Cloud Transitions over the Northern Pacific. *J. Climate*,**26**, 5761-5781.

Moeng, C.-H., 2014:: A closure for updraft-downdraft representation of subgrid-scale fluxes in cloud-resolving models. Monthly Weather Review, 142, 703–715.

Firl, G., and D. A. Randall, 2015: Fitting and Analyzing Large-Eddy Simulations Using Multiple Trivariate Gaussians. *J. Atmos. Sci.*,**72**, 1094-1116.doi: http://dx.doi.org/10.1175/JAS-D-14-0192.1.

Thayer-Calder, K., P. A. Bogenschutz, A. Gettelman, C. Craig, S. Goldhaber, C.-C. Chen, J. Höft, E. Raut, B. M. Griffin, J. K. Weber, V. E. Larson, M. C. Wyant, R. Wood, M. Wang, Z. Guo, and S. J. Ghan, 2015: A unified parameterization of convection and turbulence using CLUBB and subcolumns in the Community Atmosphere Model. *Geosci. Mod. Dev.*, submitted 5-28, revised.

Wang, M., V. Larson, S. Ghan, M. Ovchinnikov, D. P. Schanen, H. Xiao, X. Liu, P. Rasch, and Z. Guo, 2015: A Multi-scale Modeling Framework model (superparameteized CAM5) with a higher-order turbulence closure: model description and low cloud simulations. *J. Adv. Model. Earth Sys.*, 7, doi:10.1002/2014MS000375.

Xu, K.-M., and A. Cheng, 2013: Evaluating low-cloud simulation with an upgraded multiscale modeling framework model. Part I: Sensitivity to spatial resolution and climatology. *J. Climate*, **26**, 5717-5740.

Xu, K.-M., and A. Cheng, 2013: Evaluating low-cloud simulation with an upgraded multiscale modeling framework model. Part II: Seasonal variations over the Eastern Pacific. *J. Climate*, **26**, 5741-5760.

Presentations:

Bogenschutz, P. A., 2013. Improving cloud and turbulence processes in cloud resolving GCMs.

2013 AGU Fall Meeting, session on Fast Physics in Climate Models, San Francisco, CA

Bogenschutz, P. A., 2014: Cloud resolving simulations with a higher-order turbulence closure. 2014 Joint Workshop on Global Cloud Resolving Modeling and 3rd International Workshop on Nonhydrostatic Numerical Models, Kobe, Japan.

Bogenschutz, P. A. and C.-H. Moeng, 2015: Cloud resolving simulations with a a higher-order turbulence closure: scale sensitivity and aerosol effects. 2015 Atmospheric Radiation Measurement, Atmospheric System Research spring meeting, Tysons Corner, VA.

Bogenschutz, P. A. and C.-H. Moeng, 2013: Cloud resolving simulations with a higher-order turbulence closure. 2014 Atmospheric Radiation Measurement, Atmospheric System Research spring meeting, Potomac, MD.

Firl, G., and D. A. Randall, 2009: Development of a Second-order Closure Turbulence Model with Subgrid-scale Condensation and Microphysics. Paper presented at the Fall Meeting of the American Geophysical Union, San Francisco, CA.

Firl, G., and D. A. Randall, 2009: A third-order closure model. Paper presented at the Fall AGU, San Francisco.

Firl, G., and D. A. Randall, 2013: THOR: A New Higher-Order Closure Assumed PDF Subgrid-Scale Parameterization; Evaluation and Application to Low Cloud Feedbacks. Fall meeting of the American Geophysical Union, San Francisco, California, December 9-13, 2013.

Khairoutdinov, M. F., 2015: Cloud, Precipitation, and Radiation Interactions in Process Models. Invited presentaton at Gordon Research Conference, Bates College, Lewiston, ME

Khairoutdinov, M. F., 2015: Radiative-Convective Equilibrium: 1) diurnal cycle in the land-ocean system and 2) how wrong are the Grey-Zone simulations? ClimaTea Lecture, Harvard, MA

Randall, D. A., 2013: Pathways for parameterization of turbulence and shallow convection. 2013 KIAPS International Symposium, Seoul, Korea, October 28, 2013 (invited).

Randall, D. A., 2013: Clouds and turbulence. Computational Fluid Dynamics / Large Eddy Simulation Workshop, Argonne National Laboratory, Chicago, Illinois, September 4, 2013 (Invited).

Randall, D. A., 2014: Prime prime bar: Fifty years of fluxes. CMMAP Team Meeting, January 7-9, Newport Beach, California

Randall, D. A., and G. Firl, 2014: Promise and Limitations of PDF Based Parameterizations Invited. Paper presented at the *Fall Meeting of the American Geophysical Union.* (Invited)

Randall, D. A., 2014: The Importance of Third Moments. ASR Science Team Meeting, March 10-12, Bethesda, Maryland.

Randall, D. A., 2014: The small scales you will always have with you. Latsis Symposium, June18-21, Zurich, Switzerland. (Invited)